Tellus
SERIES B
CHEMICAL
AND PHYSICAL
METEOROLOGY
PUBLISHED BY THE INTERNATIONAL METEOROLOGICAL INSTITUTE IN STOCKHOLM

Tellus (2010), 62B, 389–402

TELLUS

Observation-based estimates of fossil fuel-derived CO_2 emissions in the Netherlands using $\Delta^{14}C$, CO and ^{222}Radon

By S. VAN DER LAAN[1,*], U. KARSTENS[2], R.E.M. NEUBERT[1], I.T. VAN DER LAAN-LUIJKX[1] and H.A.J. MEIJER[1], [1]*Centre for Isotope Research, Nijenborgh 4, 9747 AG Groningen, University of Groningen, Groningen, the Netherlands*; [2]*Max Planck Institute for Biogeochemistry, Jena, Germany*

(Manuscript received 4 December 2009; in final form 1 July 2010)

ABSTRACT

Surface emissions of CO_2 from fossil fuel combustion ($\Phi FFCO_2$) are estimated for the Netherlands for the period of May 2006–June 2009 using ambient atmospheric observations taken at station Lutjewad in the Netherlands (6°21′E, 53°24′N, 1 m. a.s.l.). Measurements of $\Delta^{14}C$ on 2-weekly integrations of CO_2 and CO mixing ratios are combined to construct a quasi-continuous proxy record ($FFCO_2^*$) from which surface fluxes ($\Phi FFCO_2^*$) are determined using the ^{222}Rn flux method. The trajectories of the air masses are analysed to determine emissions, which are representative for the Netherlands. We compared our observationally based estimates to the national inventories and we evaluated our methodology using the regional atmospheric transport model REMO. Based on 3 yr of observations we find annual mean $\Phi FFCO_2$* emissions of (4.7 ± 1.6) kt km^{-2} a^{-1} which is in very good agreement with the Dutch inventories of (4.5 ± 0.2) kt km^{-2} a^{-1} (average of 2006–2008).

1. Introduction

Human activities have induced global warming by emitting large amounts of the long-lived greenhouse gases carbon dioxide (CO_2), methane (CH_4), nitrous oxide (N_2O) and halocarbons. From this group, CO_2 is the largest contributor to global warming (Forster et al., 2007). To prevent global warming to rise to dangerous levels, most countries have joined an international treaty, the United Nations Framework Convention on Climate Change (UNFCCC), with the intention to reduce their greenhouse gas emissions. Currently, 184 parties of this convention have also signed the Kyoto protocol subjecting themselves to legally binding targets to reduce their emissions by on average 5% by the year 2012 (calculated as the average of 2008–2012) compared to 1990. At the 15th Conference of Parties in Copenhagen in 2009 much larger reduction targets were negotiated but a legally binding agreement could not yet be agreed upon. Nevertheless, the Netherlands declared to reduce its emissions by 30% by the year 2020 (compared to 1990) and the European Union has agreed to a reduction target of 20–30%.

Currently, these reduction targets are not validated by means of an independent approach. Parties only report their annual greenhouse gas emissions based on statistical inventories (UNFCCC, 2009), by estimating the emission or uptake of various source and sink processes, and adding them all up. However, these bottom-up statistics can potentially be biased if the emission or uptake of relevant sources or sinks are incorrect or missing. Furthermore, the uncertainties can be as large as, or even larger than, the reduction target itself (Rypdal and Winiwarter, 2001; Levin et al., 2003). In principle, the only truly independent method for verification of emission reductions is by observing the changes in the atmosphere. However, observations of CO_2 mixing ratios alone are not sufficient because of the very large natural CO_2 fluxes and secondly, the atmosphere integrates all emissions in space and time. This makes it difficult to accurately determine the magnitude of the fluxes (from surface to atmosphere or vice versa) and to aggregate them over a certain area. One commonly applied method for estimating surface fluxes from ambient mixing ratios is to combine ambient measurements with atmospheric transport models; the so-called inverse modelling method (Rayner et al., 1999; Bousquet et al., 2000; Rödenbeck et al., 2003; Bergamaschi et al., 2005; Peylin et al., 2005; Baker et al., 2006). In spite of the mathematical elegance of this method there are still large uncertainties involved regarding (e.g.) estimations of the boundary layer height, modelled transport in the atmosphere and errors related to the resolution

*Corresponding author.
Climate and Environmental Physics, Physics Institute, Sidlerstrasse 5, CH-3012 Bern, University of Bern, Switzerland.
e-mail: s.van.der.laan@rug.nl
DOI: 10.1111/j.1600-0889.2010.00493.x

of the model (Engelen et al., 2002; Rödenbeck et al., 2006; Tolk et al., 2008). Furthermore, the method is highly sensitive to measurement biases between different observation stations as these would be translated by the model into a very strong source or sink in-between. This method is therefore not (yet) suitable and is currently not applied for estimating the fossil fuel based CO_2.

A more suitable observation-based method for estimating surface fluxes is the ^{222}Radon (^{222}Rn) flux method (Levin, 1984; Thom et al., 1993; Schmidt et al., 1996). ^{222}Rn is a radioactive noble gas (its half-life time is 3.8 d) that is produced at a constant rate from ^{226}Radium, which is relatively uniformly distributed in all soils. When released into the atmosphere, ^{222}Rn experiences the same atmospheric circumstances (i.e. transport and dilution through mixing) as all other gases released from the surface. If the Rn flux is known and its atmospheric concentration measured, the ratio between those two can be determined, and subsequently applied to calculate surface fluxes from mixing ratios of other gases in the atmosphere. The main condition for using this method is that the ^{222}Rn soil emission has to be well known in time and space. This method has been applied successfully to estimate the emissions of CH_4 and N_2O in the Netherlands (Van der Laan et al., 2009b). In this paper, we will demonstrate the method for CO_2 emissions from fossil fuel combustion.

After a description of our measurement site Lutjewad and the equipment used (Section 2), we will describe the use of the radioactive isotope ^{14}C to identify the CO_2 from fossil fuel combustion ($FFCO_2$) in Section 3.1. Since CO_2 from fossil fuels contains no ^{14}C anymore due to its high age, ^{14}C can be used as a proxy for fossil fuel CO_2 emissions (Levin, 1987; Zondervan and Meijer, 1996; Turnbull et al., 2006). Because ^{14}C is too labour intensive to allow continuous observations, we apply a second tracer: Carbon Monoxide (CO). CO has proven to be a valuable proxy for $FFCO_2$ (Meijer et al., 1996; Levin et al., 2003; Gamnitzer et al., 2006; Turnbull et al., 2006) as its sources are very closely linked to that of $FFCO_2$. Any hydrocarbon oxidation process with CO_2 as an end product is to some extent associated with CO production (Gamnitzer et al., 2006). We therefore calibrate our carbon monoxide (CO) mixing ratios to $FFCO_2$, which are integrated samples over 2 weeks, and construct a high-resolution proxy for fossil fuel derived CO_2 ($FFCO_2$*). We subsequently apply the ^{222}Rn flux method to calculate the surface emissions $\Phi FFCO_2$* (Section 3.2) and make a distinction between Dutch emissions and emissions from abroad by looking at their trajectories. Similarly, we distinguish between emissions from the northern part of the Netherlands (where station Lutjewad is located) and emissions from the densely populated centre and southern part from where we expect the highest emissions. For comparison, and for testing the methodology, the same exercise was performed on modelled concentrations of ^{222}Rn and $FFCO_2$ from the regional transport model REMO (Section 3.3). Finally, the results are compared to the national inventories (Section 4).

2. Measurement site Lutjewad and applied instrumentation

All measurements were performed at our station Lutjewad (53°24′18″N, 6°21′13″E, 1 m above sea level). The station is located in the north of the Netherlands on the Dutch North Sea coast, about 30 km to the northwest of the city of Groningen. Measurements include quasi-continuous observations of CO_2, CH_4, N_2O, SF_6, CO and ^{222}Radon, automated flask sampling (^{13}C, ^{14}C, O_2/N_2, CO_2, CH_4, CO), Eddy covariance (CO_2, H_2O) and basic meteorological properties (air temperature, humidity, atmospheric pressure, wind-speed and direction and solar radiation). See also Neubert et al. (2004). Wind conditions at the site are such that most air is sampled from wind directions between southwest to west. During the period of May 2006–May 2009 the prevailing wind direction (31%) was between 195° and 255° and most wind speeds (35%) were between 6 and 9 m s^{-1}, based on observations at 60 m above ground level (the same as the sample intake) (Van der Laan et al., 2009b). The majority of the sampled air in Lutjewad is therefore highly influenced by emissions from the Netherlands.

From the intake at a height of 60 m, air is flushed down continuously to a laboratory where the air is dried to a dew point of −50 °C, after which the analyses take place and the air is collected in flasks.

Following a travel time of about 4 min the sample air is fed to a modified Agilent HP 6890N Gas Chromatograph (GC) where separation and analyses of CO_2 and CO (also CH_4, N_2O and SF_6) take place. About six measurements are performed in 1 h and the obtained measurement uncertainty is about ±0.04–0.06 ppm for CO_2 and 0.8–1.8 ppb for CO (Van der Laan et al., 2009a).

Bi-weekly integrated samples of CO_2 are collected by absorption of CO_2 in CO_2-free sodium hydroxide (NaOH) solutions. $\Delta^{14}C$ is then determined by conventional ^{14}C analysis, or in the case of small samples due to unfavourable wind conditions, in duplicate with Accelerator Mass Spectrometry (AMS) in our radiocarbon laboratory in Groningen (Stuiver and Polach, 1977; Mook and Van der Plicht, 1999). For this study, samples were collected only when wind direction was between 100° and 250° in order to sample continentally influenced emissions. The measurement precision is typically ±2–3 ‰ for both methods.

Ambient concentrations of ^{222}Rn are measured (half hourly averages) with an ANSTO dual-flow loop two-filter detector (Whittlestone and Zahorowski, 1998). The total travel time from the inlet in the mast, at 60 m height, is about 10 min. The detector is a non-energy selective alpha particle counter and would detect ambient ^{220}Rn (half-life time of 55.6 s) as well as ^{222}Rn. However, this is prevented because of the relatively long travelling time from the tower inlet to the detector compared to the decay of ^{220}Rn, that is, roughly 10 half life times. A filter in front of the detector removes aerosols and (radioactive) decay products. The ^{222}Rn decay products are sampled on a second filter in a 1500 litre delay chamber, where their decays

are counted by a photo-multiplier. The combined measurement uncertainty depends on the total decay counts and the uncertainty of the ^{222}Rn source with which the device is calibrated, and is typically 5%.

3. Method

3.1. Constructing a quasi-continuous proxy for CO_2 from fossil fuels

Our first step is to identify the 2-weekly integrated CO_2 from fossil fuels ($FFCO_2$) by combining our semi-continuous CO_2 mixing ratios with the 2-weekly integrated $\Delta^{14}C$ measurements. We subsequently calibrate carbon monoxide (CO) to $FFCO_2$ to obtain a high-resolution proxy for $FFCO_2$ ($FFCO_2{}^*$), which is needed for estimating the Dutch surface emissions of CO_2 from fossil fuels.

Ambient observed mixing ratios of CO_2 (CO_{2obs}) consist of a background component (CO_{2bg}), a fossil fuel component ($FFCO_2$), a biosphere component (CO_{2bio}) and an oceanic component (CO_{2oc}). In our case we include CO_{2oc} in CO_{2bg} since we assume the $\Delta^{14}C$ gradient between Lutjewad and Jungfraujoch (which we use as a background reference station) is negligible. This gives

$$CO_{2obs} = CO_{2bg} + CO_{2bio} + FFCO_2. \quad (1)$$

Expressed in $\Delta^{14}C$, which is the ratio of $^{14}C/^{12}C$ per mille deviations from the standard pre-industrial atmosphere and corrected for radioactive decay and mass dependent fractionation (Stuiver and Polach, 1977), gives

$$\begin{aligned} CO_{2obs}(\Delta^{14}C_{obs} + 1) = {} & CO_{2bg}(\Delta^{14}C_{bg} + 1) \\ & + CO_{2bio}(\Delta^{14}C_{bio} + 1) \\ & + FFCO_2(\Delta^{14}C_{ff} + 1), \end{aligned} \quad (2)$$

where the bio-term includes both respiration and photosynthesis. As the ^{14}C in fossil fuels is already decayed, $\Delta^{14}C_{ff} = -1$ according to its definition, and thus the final term on the right is zero. This leads to

$$FFCO_2 = \frac{CO_{2bg}\left(\Delta^{14}C_{bg} - \Delta^{14}C_{bio}\right) - CO_{2obs}\left(\Delta^{14}C_{obs} - \Delta^{14}C_{bio}\right)}{\Delta^{14}C_{bio} + 1}. \quad (3)$$

Following Meijer et al. (1996) and Zondervan and Meijer (1996) we set $CO_{2bio} = CO_{2bg}$ in eq. (3) which gives

$$FFCO_2 = CO_{2obs} \cdot \frac{\left(\Delta^{14}C_{obs} - \Delta^{14}C_{bg}\right)}{\Delta^{14}C_{bg} + 1} + \varepsilon_{resp}. \quad (4)$$

The biosphere component (CO_{2bio}) consists of about 50% of autotrophic respiration, which is in close equilibrium with the background (Levin et al., 2008). The heterotrophic respiration should in principle be taken into account for terrestrial sites (Randerson et al., 2002) but is due to the large heterogeneity of the biosphere difficult to estimate precisely (e.g. Levin et al., 2003; Gamnitzer et al., 2006; Graven et al., 2009). Based on a mean terrestrial residence time of 10 yr Turnbull et al. (2006) estimated for the northern hemisphere that $FFCO_2$ would be underestimated due to this biospheric $^{14}CO_2$ source between 0.2 ppm in winter to 0.5 ppm in summer. In this study we therefore add a harmonic regression fit between 0.2 ppm in winter and 0.5 ppm in summer to our $FFCO_2$ values from eq. 4 (ε_{resp}) as an approximation for the seasonal $^{14}CO_{2bio}$ effect on $FFCO_2$.

Because $^{14}CO_2$ is constantly produced in the upper atmosphere, the ideal background reference $\Delta^{14}C_{bg}$ would be sampled at a station low enough to avoid variations caused by changes in the production rate (e.g. changes in cosmic radiation intensity) but high enough from the earth's surface to avoid depletion of its mixing ratio by fossil fuel CO_2 emissions (Hesshaimer, 1997; Randerson et al., 2002). The High Alpine site Jungfraujoch (JFJ) (3450 m a.s.l.) in the Swiss Alps (Levin et al., 2003; Levin et al., 2008) is about the best practical realisation available of this ideal situation, so we used the $\Delta^{14}C$ observations of JFJ as a background reference fitted with a linear trend fit with a 1-harmonic seasonality.

The 2-weekly integrated $\Delta^{14}C$ mixing ratios from our NaOH-based CO_2 sampler at Lutjewad, as well as the JFJ $\Delta^{14}C$ measurements for the period of May 2006–May 2009 are shown in Fig. 1a together with the Dutch monthly mean temperature (source: www.KNMI.nl). Very low $\Delta^{14}C$ values are observed in the (very cold) winter of 2008–2009, compared to the previous years. An extremely low $\Delta^{14}C$ value of -6.4% was measured in the first 2 weeks of January 2009 indicating high influence of fossil fuel burning and low atmospheric mixing. Fig. 1b shows the corresponding 2-weekly averaged $FFCO_2$ mixing ratios as calculated with eq. (4) and corrected for $\Delta^{14}C_{bio}$. The regression fit, a LOESS weighted smooth with a smoothing factor set to 1 yr, illustrates the clear seasonal pattern but does not capture the very low and high excursions. High $FFCO_2$ mixing ratios are generally observed in the winter and lower values in the summer, both influenced by atmospheric conditions (i.e. transport and planetary boundary height) as well as anthropogenic activity. The very low $\Delta^{14}C$ excursion of -6.4% in Fig 1a is shown as a very high $FFCO_2$ mixing ratio of 20.6 ppm. The seasonal amplitudes vary strongly between the years with about 4 ppm in 2006 to about 9 ppm in 2009. The lower values are attributed to the fact that the year 2006 was a very warm year; the winter of 2006–2007 was the warmest in the Netherlands since at least 300 yr (KNMI, 2009). The uncertainty in the $FFCO_2$ observations is typically 1.4 ppm. The corresponding relative error is around 20% for most observations, but can become much larger (i.e. $>100\%$) when the $\Delta^{14}C$ observations are close to the JFJ reference (i.e. very low $FFCO_2$).

For practical reasons ($\Delta^{14}C$ measurements are too costly and time- and labour-intensive to allow high resolution) our $\Delta^{14}C_{obs}$

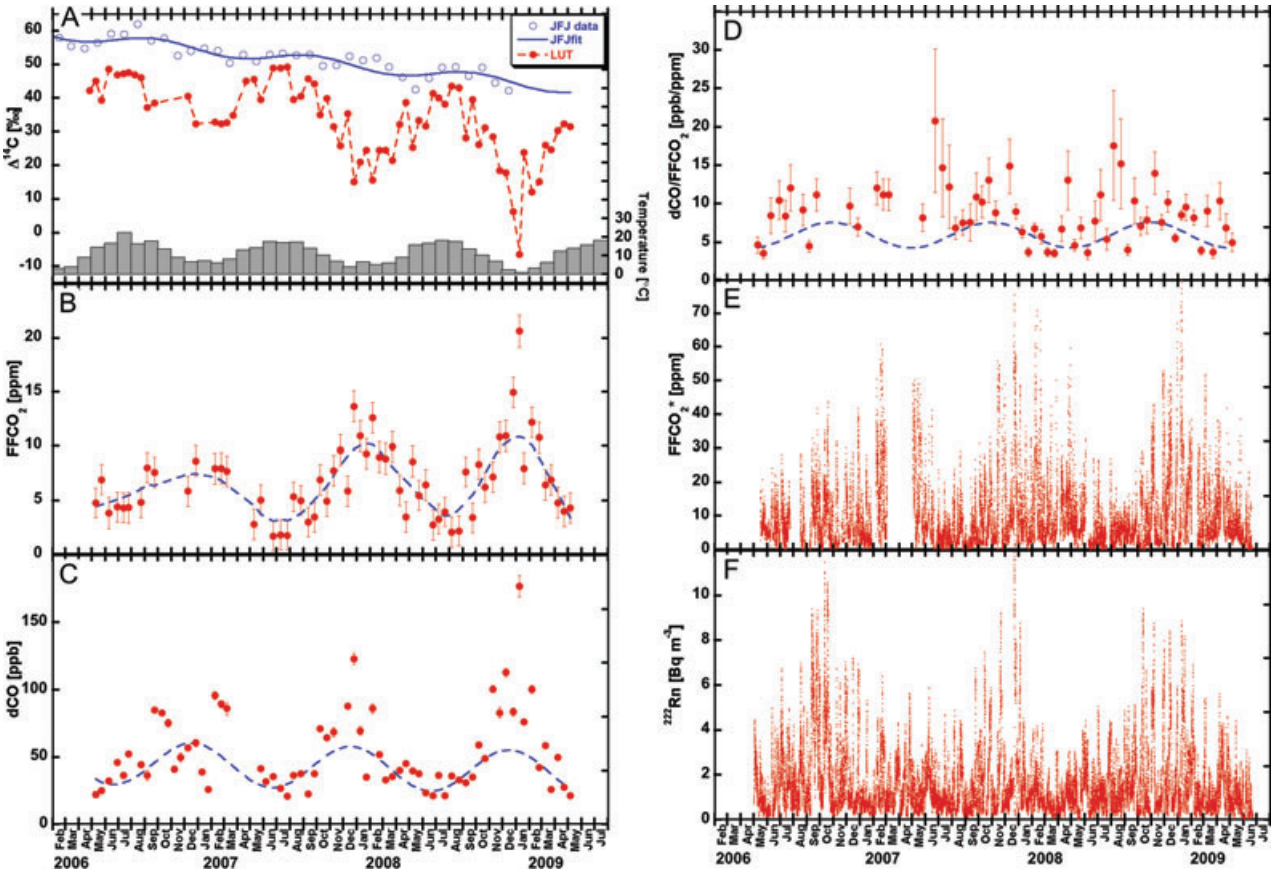

Fig. 1. (a) Jungfraujoch $\Delta^{14}C$ data with a linear trend fit and a 1-harmonic seasonal cycle which is used as a background and our 2-weekly integrated $\Delta^{14}C$ data from Lutjewad's south sector from May 2006 to June 2009. (b) $FFCO_2$ (corrected for biospheric ^{14}C) calculated from eq. (4) with a linear trend fit and a 1-harmonic seasonal cycle. (c) Two-weekly dCO mixing ratios fitted with a weighted linear trend fit with a 1-harmonic seasonality (only to guide the eye). (d) $dCO/FFCO_2$ ratio fitted with a weighted linear trend fit with a 1-harmonic seasonality (e) High resolution $FFCO_2{}^*$ mixing ratios calculated as described in Section 3.1. (f) ^{222}Rn observations for the same period.

(and thus $FFCO_2$) are limited to 2-weekly integrated samples. Therefore, we calibrated our (2-weekly integrated) high resolution CO mixing ratios to 2-weekly integrated $FFCO_2$ and convert our CO data set to a proxy for $FFCO_2$ which is defined here as: $FFCO_2{}^*$. First, we determined a background for CO by fitting the daily minimum values with a weighted mean, and subtracted it from the CO mixing ratios in order to determine the CO enhancements from the background (dCO). Fig. 1c shows the 2-weekly integrated dCO observations, fitted with a weighted linear trend fit with a harmonic seasonality to guide the eye. The high excursions from the background value, which are observed in the winters, are not well represented by the fit. For each 2 week-integrated sample $\Delta^{14}C_{obs}$ we calculated a ratio $dCO/FFCO_2$ which is shown in Fig. 1d. Most observed values are between 5 and 15 ppb $dCO/FFCO_2$ ppm. This low ratio is related to the high share of natural gas in fossil fuel consumption in the Netherlands (Meijer et al., 1996) which is used for a major part of the electricity production and for almost all heating of buildings. The seasonal cycle of $dCO/FFCO_2$ is therefore mainly temperature driven. In the winter periods, the fossil fuel emissions in the Netherlands are dominated by the heating of buildings which decreases the ratio $dCO/FFCO_2$ because very little carbon monoxide is formed when combusting natural gas. Because of the high variability and often large error bars, the data were fitted with a weighted linear trend fit with a harmonic seasonality which was used to convert the CO mixing ratios to $FFCO_2{}^*$. This fit is mainly determined by observations from mid 2007-mid 2009, as there are fewer observations in the first year due to technical difficulties. The fit is also in lesser extent influenced by the observations in the summer where the uncertainty is generally very large. Figure 1e shows the high resolution mixing ratios of $FFCO_2{}^*$ which also have a clearly seasonal cycle with higher mixing ratios in the winter periods and lower values in the summers. The ^{222}Rn observations for the corresponding period are shown in Fig. 1f. Higher concentrations are generally observed in the winters when the atmosphere is more stable.

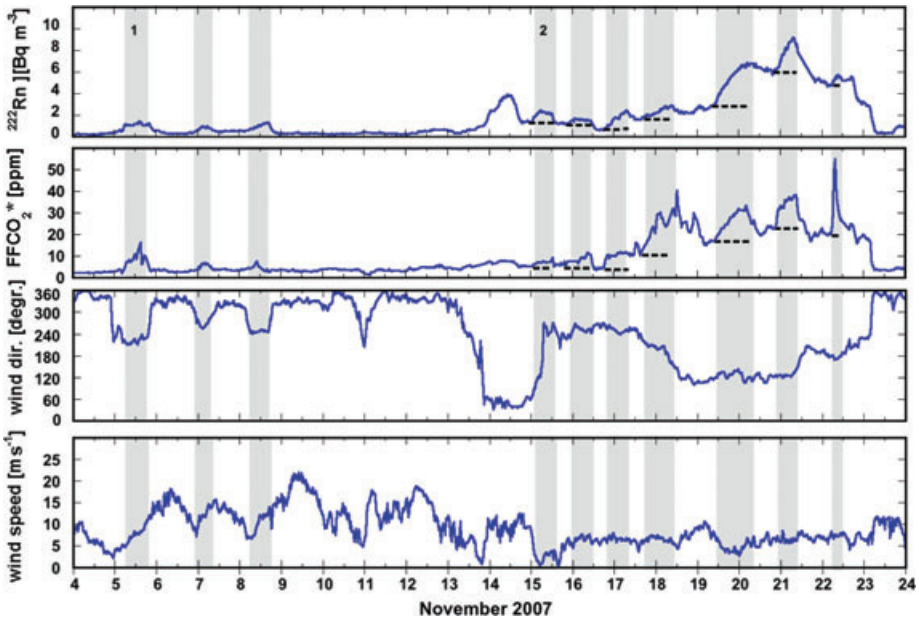

Fig. 2. Example of the different types of events (shaded areas) observed at station Lutjewad. Three typical short-range events (the first indicated with 1) starting at November 5 show an increase of ^{222}Rn concentrations from baseline levels. The marked events starting at November 15 (the first is marked with a 2) are built up on a slow increase in the ^{222}Rn concentration, which indicates a persistent continental influence. These events are treated as short-range events after a new baseline is defined (dotted lines) for each individual event.

3.2. Event selection

To calculate surface fluxes from $FFCO_2^*$ ($\Phi FFCO_2^*$) and distinguish between different source areas, we selected the data based on specific events according to the build-up of ^{222}Rn in the atmosphere which is common with stable atmospheric conditions. Figure 2 shows an example of some of these events, indicated with shaded areas, observed at our station from November 4 to November 24 in the year 2007. We selected an event when a significant departure of ^{222}Rn from the background concentrations was observed for at least four consecutive hours. Due to lack of vertical mixing with free tropospheric air, all surface emissions (e.g. ^{222}Rn and $FFCO_2$) are trapped in the lower atmospheric boundary layer. An event terminates when vertical mixing is re-established. Events which start already before background level is regained (indicating a long period of continental influence, indicated with the number 2 in Fig. 2) are treated similarly to the other events after defining a new baseline (illustrated by the dashed lines). Similarly to Van der Laan et al. (2009b) we assume that the meteorological circumstances (e.g. wind speed) remain stable and the transit time is the same for the whole air mass, and use the length of an event as an indicator for the area of influence.

We analysed the trajectories of the air masses with the Hysplit 4 lagrangian back trajectory model (Draxler and Rolph, 2003) using hourly Global and hourly Data Assimilation System (GDAS) metrological data (downloadable from http://ready.arl.noaa.gov/gdas1.php) for each event corresponding to the total duration of the event. For example, if an event sustained for 8 h we calculated a trajectory 8 h back in time. As a starting point we used the last data point of an event (before vertical mixing was re-established) as well as a point in the middle of an event in order to validate steady-state conditions during travel. Events were accepted for further analysis if the trajectories indicated that the track of the air mass was mainly (>70%) over the Netherlands in order to select events, which were dominantly influenced by Dutch emissions.

Figure 3 shows a contour plot constructed from the hourly points on the trajectories of all events which were selected for further analysis. The values are normalized towards the end points of the trajectories (station Lutjewad, indicated with an "x") in order to show the relative sampling density over the footprint. Each event represents the average surface emissions along its trajectory, while the effective capture range around such a trajectory gets broader the further one goes back in time. Therefore, to determine the mean emissions of the Netherlands we would only have to collect a series of events that together represent the total area of the Netherlands, implying that such trajectories would have to start close to the borders of the country. Attributing the same weight to trajectories that start close(r) to our station as to those further reaching ones would lead to an overrepresentation of the region close to the station, which is also clear from Fig. 3. As a practical solution, we decided to divide the country into two sectors: the first relatively close (∼100 km radius) to the station (sector 1 in Fig. 3), and the second comprising the rest of the Netherlands (sector 2 in Fig. 3).

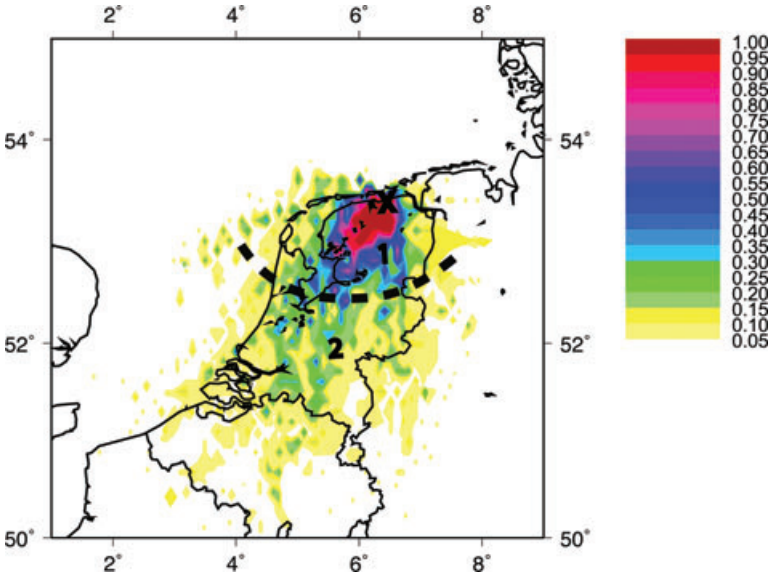

Fig. 3. Density of the selected observations over the footprint based on hourly points of back trajectories. Data is normalized to the end points of the trajectories (i.e. Lutjewad) to illustrate the relative distribution of the observations to the footprint. Station Lutjewad's location is indicated with an 'x'. Two sectors (1 and 2), based on population density are also indicated.

We then assume the trajectories starting in the outer sector to be representative for the Netherlands as a whole, whereas those starting in the inner sector would represent the regional emissions of the north of the Netherlands. The emissions from sector 2 itself are then calculated in a straightforward way from them. The two sectors are also representative for the population density in the Netherlands with sector 1 having less than 250 inhabitants km^{-2} whereas the average of the whole country is about 500 inhabitants km^{-2}. Once this separation has been made, the calculation of the flux is just the arithmetic mean of the flux results for the individual events. Accordingly, the uncertainty is the square root of the quadratic sum of individual event uncertainties, divided by the number of events.

3.3. Calculation of $\Phi FFCO_2{}^*$ surface fluxes

To calculate the surface fluxes, linear regression fits were made for each selected event. An example of a regression fit between $FFCO_2{}^*$ and ^{222}Rn for a single event, which was observed from 13 August 2006 18:30 UTC to 7:00 UTC the next day, is shown in Fig. 4. ^{222}Rn increased by about 2 Bq m^{-3} during this period and $FFCO_2{}^*$ by about 9 ppm. The correlation (assumed by the ^{222}Rn flux method) between $FFCO_2{}^*$ and ^{222}Rn was significant: $R = 0.9$. For the regression slopes a correlation coefficient of $R \geq 0.7$ is used as a threshold for further analysis. Hereby we aim to maintain regression slopes with a sufficient correlation and still have enough events to determine annually averages. In total 184 events were selected with 97 from sector 1 and 87 from sector 2.

The surface flux $\Phi FFCO_2{}^*$ for each event is calculated as follows (Levin, 1984; Thom et al., 1993; Schmidt et al., 1996)

$$\overline{\Phi}_{FFCO_2*} = \overline{\Phi}_{Rn} \cdot \frac{\Delta FFCO_2{}^*}{\Delta Rn}, \tag{5}$$

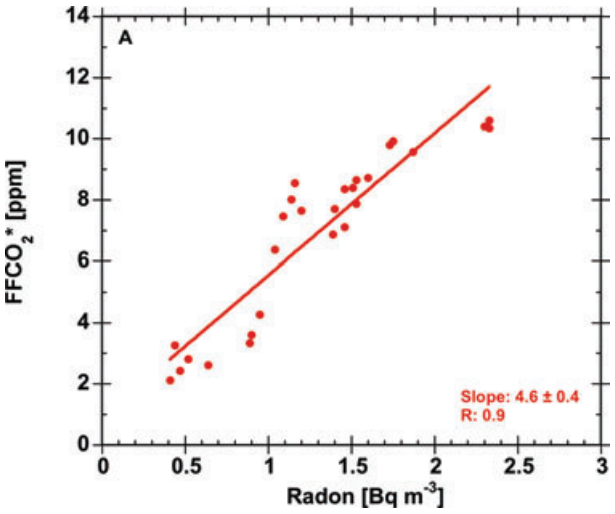

Fig. 4. $FFCO_2{}^*$ and ^{222}Rn determined from a single event starting at 13 August 2007 18:00 UTC and ending at 7:00 UTC the next day.

where Φ_{FFCO_2*} represents the surface flux of $FFCO_2{}^*$, Φ_{Rn} is the ^{222}Rn soil flux rate, $FFCO_2{}^*$ represents the atmospheric mixing ratios of $FFCO_2{}^*$ and Rn is the atmospheric concentration of $^{222}Radon$. The overbars are the means for the spatial and temporal scales of influence. The Δ's represent enhancements from their background values. Hence, the second term in eq. 5 is the linear regression fit for each event. Basically, an atmospheric transport coefficient is determined from the ratio of the ^{222}Rn soil flux rate to the observed ^{222}Rn concentrations at a certain height. The mixing ratios of $FFCO_2{}^*$, if measured at the same height, can then be scaled to its surface flux ($\Phi FFCO_2{}^*$) assuming the atmospheric transport and dilution (e.g. by mixing with the free troposphere under unstable atmospheric conditions) is the same. As explained above, the radioactive noble gas ^{222}Rn is

suitable for this application. However, since ^{222}Rn is subjected to radioactive decay we have to correct for this. Similarly to Van der Laan et al. (2009b) we assume that the transit time is the same for all air masses which are collected during one event and correct our $\Phi FFCO_2{}^*$ results for the ^{222}Rn decay by multiplying eq. (5) with:

$$\frac{\int_0^{\tau_{max}} e^{-\lambda\tau} d\tau}{\tau_{max}} = \frac{-\lambda^{-1}\left(e^{-\lambda\tau_{max}} - 1\right)}{\tau_{max}} = \frac{1 - e^{-\lambda\tau_{max}}}{\lambda\tau_{max}}, \quad (6)$$

wherein τ_{max} represents the maximum transit time for the specific observation period, for which we take the total length of each event, and λ is the decay constant (0.182 d^{-1}) of ^{222}Rn. In this study, the applied correction for radioactive decay was on average <5%.

For both sectors we used the ^{222}Rn soil flux (Φ_{Rn}) based on a 0.5° × 0.5° ^{222}Rn soil flux map for Europe (Szegvary et al., 2009) with a temporal resolution of 1 week. Szegvary et al. (2009) constructed this map, based on the correlation between ^{222}Rn and gamma-dose rate measurements based on observations in the year 2006. The annual mean ^{222}Rn soil flux was 0.29 atoms cm^{-2} s^{-1} for sector 1 and 0.35 atoms cm^{-2} s^{-1} in the case of sector 2. A very small seasonal cycle is present of about 0.01 atoms cm^{-2} s^{-1} with higher emissions in the summer and lower in the winter. The data was fitted with a weighted LOESS fit which we used for calculating the $\Phi FFCO_2{}^*$ emissions (Fig. 5).

3.4. $\Phi FFCO_2$ surface emissions from modelled mixing ratios

To investigate our method's sensitivity towards emissions from sector 1 and 2 we performed the same exercise on modelled mixing ratios for the year 2007 from the regional atmospheric transport model REMO (Langmann, 2000). Mixing ratios of $FFCO_2$ and ^{222}Rn concentrations were simulated by REMO for station Lutjewad and from them $\Phi FFCO_2$ surface fluxes were calculated using the approach described in this paper for sector 1 and 2. The results are then compared to the a priori, annual mean fluxes for both sectors (Fig. 6). REMO has

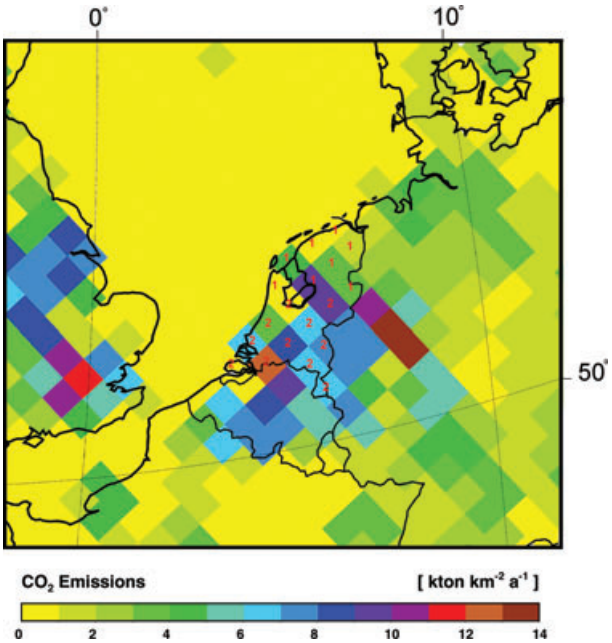

Fig. 6. REMO grid cells with emissions for the year 2007 based on the EDGAR3.2FT2000 database and BP statistics. Also indicated are the sectors representing sectors 1 and 2 from Fig. 3.

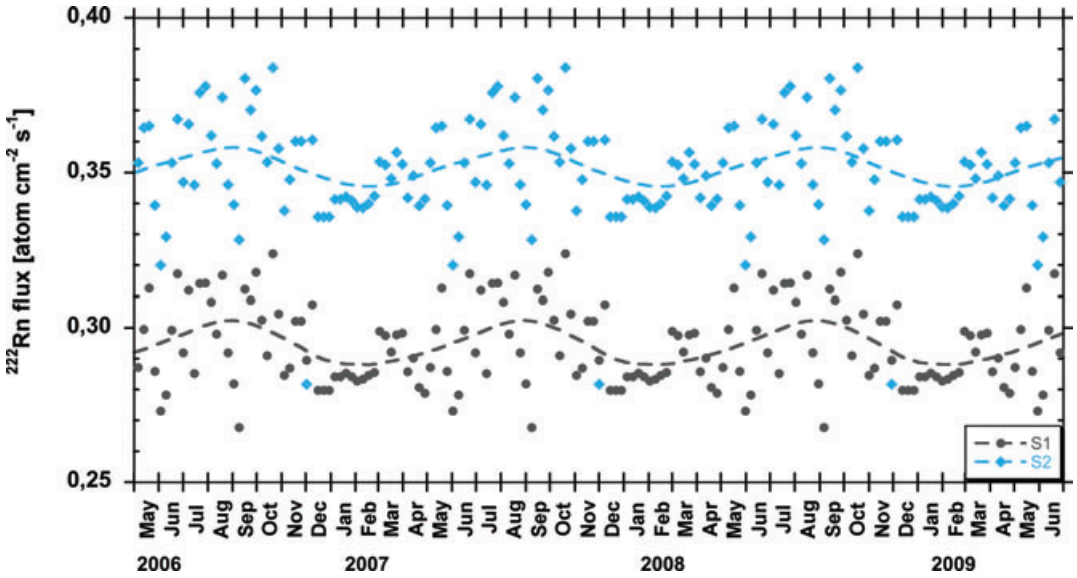

Fig. 5. ^{222}Rn soil flux rate (expressed in atom cm^{-2} s^{-1}) for both sectors based on Szegvary et al. (2009). The data was fitted with a weighted LOESS to calculate the surface fluxes $\Phi FFCO_2{}^*$.

a grid resolution of 0.5° × 0.5° in a rotated spherical coordinate system and was run on a semi-hemispheric domain covering the area north of 30N. For this study, REMO was fed with hourly $\Phi FFCO_2$ emissions based on 1° × 1° data available from the Emission Database for Global Atmospheric Research (EDGAR3.2FT2000) (Olivier et al., 2005). The emission data were extrapolated from the year 2000 to 2007 by C. Gerbig (personal communication, 2009) using BP statistics (downloadable from www.BP.com/statisticalreview) and seasonal to diurnal variations were included based on time profiles available in the EDGAR database.

The ^{222}Rn soil flux was taken from the European map given by Szegvary et al. (2009) and has a temporal resolution of 1 week and a spatial resolution of 0.5° × 0.5°. This is the same source as used for the analysis of the observations (Fig. 5). Figure 7a shows the ^{222}Rn concentrations for the Lutjewad observations and the simulations using REMO/Szegvary for January–April 2007. The synoptic variations are very well captured by the model. Figure 7b shows the correlation between the ^{222}Rn concentrations from REMO/Szegvary and our observations for all selected events for the year 2007. The correlation between the two is good ($R = 0.85$) which suggests that the a priori ^{222}Rn soil flux map from Szegvary et al. (2009) is representative for the footprint of station Lutjewad. There is, however, a large scatter in the data, which may be related to the modelled atmospheric transport and/or the limited spatial resolution of the soil flux input data.

4. Results

Figure 8 shows the results for the $\Phi FFCO_2$* surface fluxes for both sectors for the period of May 2006–June 2009. The error bars represent the uncertainty in the linear regressions fits of the events only. The harmonic regression fit to the sector 2 points is

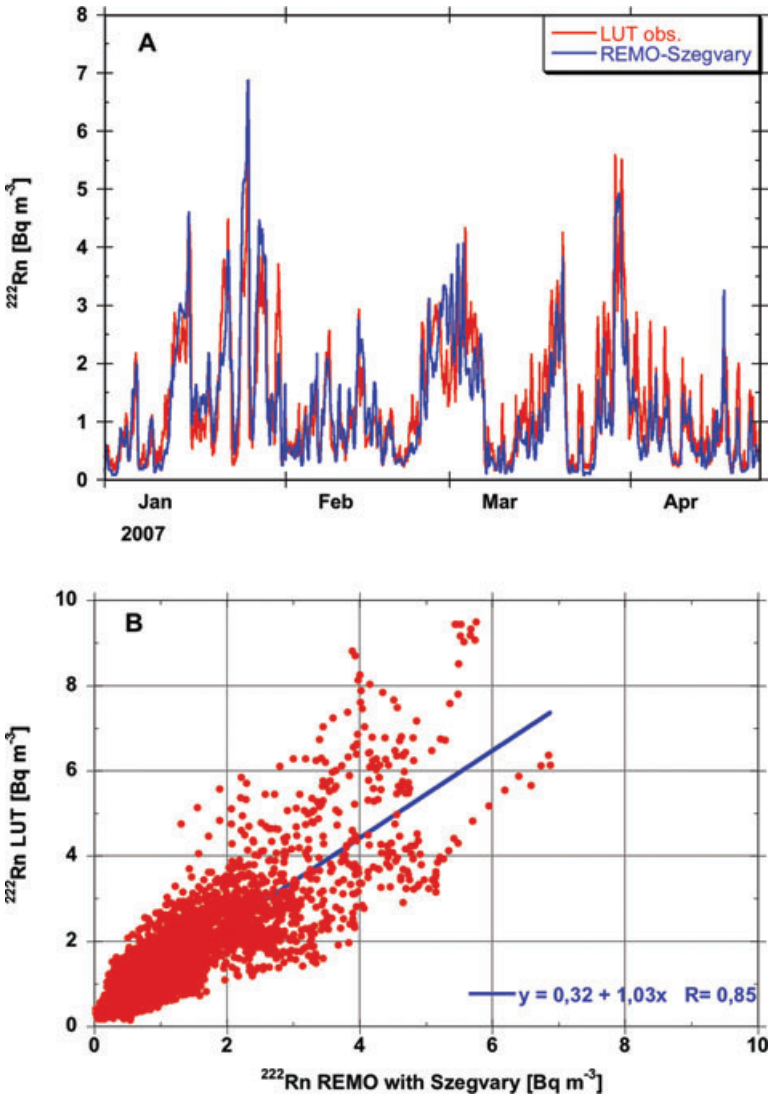

Fig. 7. (a) Comparison between ^{222}Rn observations from Lutjewad and modelled ^{222}Rn concentrations from REMO using ^{222}Rn soil emissions taken from Szegvary et al. (2009) for part of the year 2007. (b) Correlation between ^{222}Rn events from observations from Lutjewad and from REMO/Szegvary ^{222}Rn concentrations for 2007.

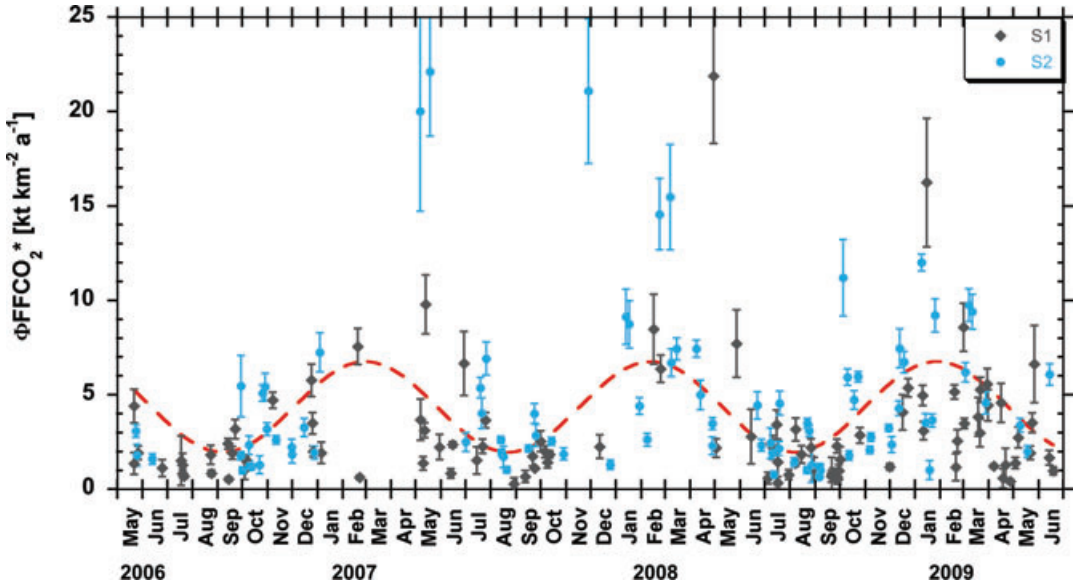

Fig. 8. $\Phi FFCO_2{}^*$ surface fluxes for the Netherlands for the period of May 2006–June 2009 fitted with a harmonic regression fit (to guide the eye). Emissions from sector 1 are generally lower then those including also emissions from sector 2. The error bars represent the uncertainties of the linear regression fits. A seasonal cycle is clearly present with lower emissions in the summer period compared to the winter.

to guide the eye only. A large variation is present in the fluxes but in general the lowest fluxes are observed in the summers and the highest in the winters. Most fluxes are observed from June 2008 to June 2009 because of wind conditions: fewer events are flagged out as being not representative for sector 1 or 2. For the period of June 2006–July 2007 44 fluxes are observed, for the period of June 2007–July 2008 47 fluxes are observed and for the period of June 2008–July 2009 84 fluxes are observed. There are too few observations to determine the annual mean emissions per year. As expected based on the population density distribution, fluxes from sector 1 are generally lower then those from sector 2. The frequency distributions of the fluxes for all observations are shown in Figs. 9a, b (for the trajectories starting within section 1) and c (for those starting within sector 2). The results for the REMO based data are shown in Figs. 9d (all observations), 9e (sector 1) and f (sector 2). As explained in Section 3.2 we consider the emissions based on trajectories starting in sector 2 as representative for the emissions of the Netherlands whereas those starting in sector 1 represent the local emissions. The annual mean emissions representative for sector 2 itself are calculated by subtracting the local emissions for sector 1 from the total emissions, by taking 19 grid cells for the Netherlands, 11 grid cells for sector 2 and 8 grid cells for sector 1 (Fig. 6).

For the total period of May 2006–June 2009 we find annual mean $\Phi FFCO_2{}^*$ surface fluxes for the Netherlands (i.e. represented by emissions starting from sector 2) of: (4.7 $\pm$ 1.1) kt km^{-2} a^{-1}. For sector 1 we find: (3.3 $\pm$ 1.1) kt km^{-2} a^{-1} and this leads to (5.7 $\pm$ 1.1) kt km^{-2} a^{-1} for sector 2. For the REMO exercise we compare our results with the emission input into REMO for both sectors as indicated in Fig. 6. Using our approach we find annual mean $\Phi FFCO_2$ surface fluxes for the Netherlands of: (4.5 $\pm$ 0.4) kt km^{-2} a^{-1}, for sector 1 of (3.3 $\pm$ 0.6) kt km^{-2} a^{-1} and then (5.4 $\pm$ 0.6) kt km^{-2} a^{-1} for sector 2. These are in very good agreement with the input fluxes of: 2.9 kt km^{-2} a^{-1} for sector 1, 5.8 kt km^{-2} a^{-1} for sector 2 and 4.6 kt km^{-2} a^{-1}for the Netherlands in total. Hence: the ^{222}Rn flux method on the modelled concentrations of ^{222}Rn and $FFCO_2$ returns the input fluxes for both sectors. This is strong support for our chosen methodology: combining $FFCO_2{}^*$ and ^{222}Rn observations with the presented analysis based on the selection of emission 'events' and back trajectory selection. Our methodology shows that using data from our station Lutjewad, emissions from both sectors and thus the Netherlands as a whole can be determined, provided a satisfactory number of 'events' with suitable back trajectories is available. All results, including our analysis with the modelled data from REMO, are summarized in Table 1.

5. Discussion

In this paper, we estimated the annual mean emissions of CO_2 from fossil fuels ($\Phi FFCO_2{}^*$) using the ^{222}Rn flux method on specific events which are selected based on their trajectories. In cases such as this one, it is common practice, but incorrect, to treat the data as shown in Fig. 9 as a normal or lognormal distribution with a single "true" value while the variability of the data is assumed to be caused by measurement and other random uncertainties. On the contrary, each measurement is the flux result for the specific area sampled by the air masses at that

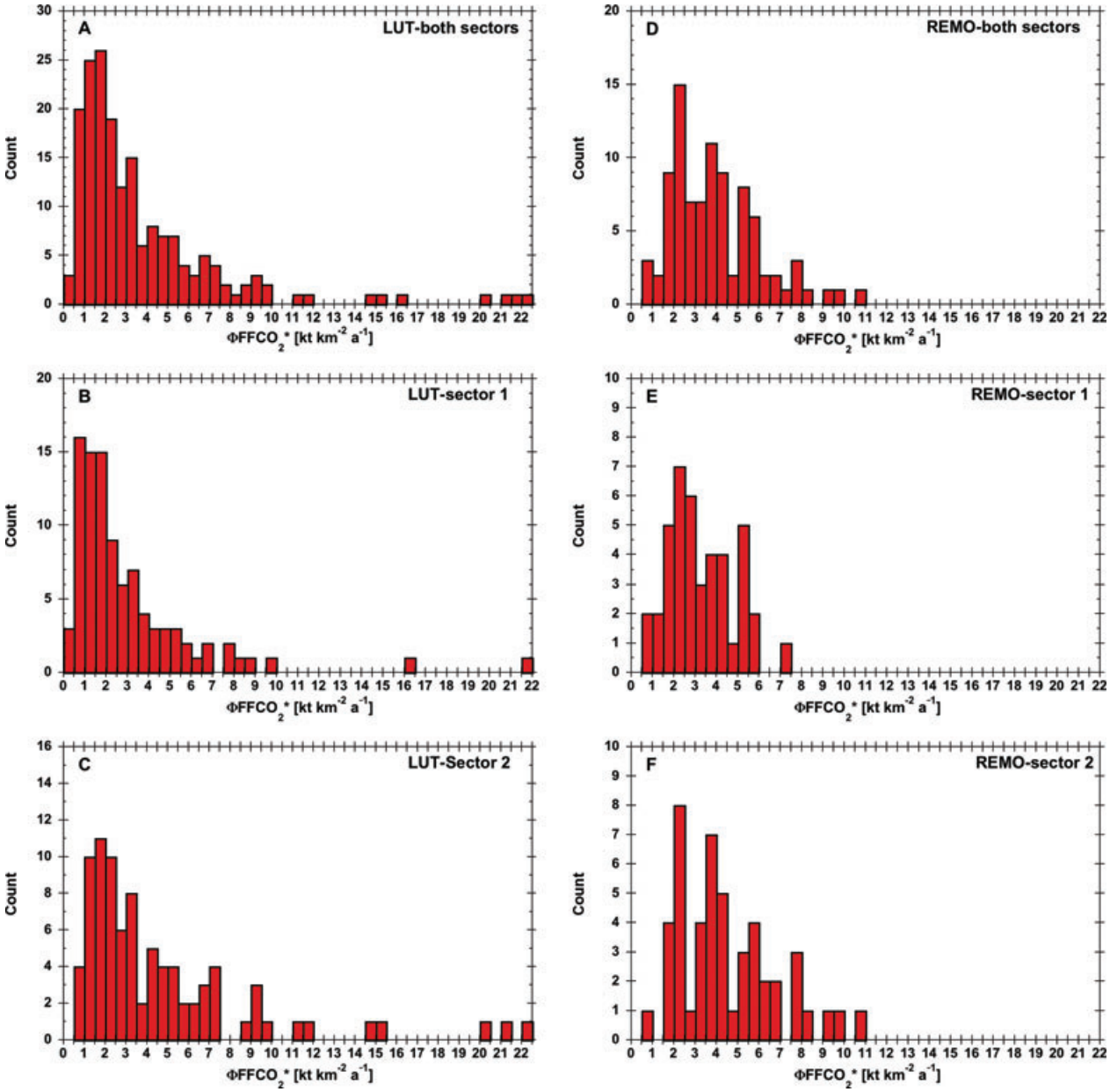

Fig. 9. (a) Frequency distribution of $\Phi FFCO_2{}^*$. (b) $\Phi FFCO_2{}^*$ for sector 1. (c) $\Phi FFCO_2{}^*$ for sector 2. (d) Frequency distribution of the $\Phi FFCO_2{}^*$ from REMO/EDGAR. (e) $\Phi FFCO_2{}^*$ REMO/EDGAR for sector 1. (f) $\Phi FFCO_2{}^*$ REMO/EDGAR for sector 2.

Table 1. Results for $\Phi FFCO_2{}^*$ and $\Phi FFCO_2$ (REMO) emissions for the Netherlands and per individual sector

	Number of events	$\Phi FFCO_2$ a priori 2007 (EDGAR3.2+ BP-statistics)	$\Phi FFCO_2$ Flux method 2007 (REMO with EDGAR3.2)	National inventory 2006–2008	$\Phi FFCO_2{}^*$ Flux method Observations Combined uncertainty May 2006- June 2009	
Sector 1 [8 grid boxes]	97	2.9	3.3 ± 0.2		3.3 ± 1.1	(kt km^{-2} a^{-1})
Sector 2 [11 grid boxes]	87	5.8	5.4 ± 1.1		5.7 ± 2	(kt km^{-2} a^{-1})
The Netherlands	87	4.6	4.5 ± 0.3	(4.5 ± 0.2)	4.7 ± 1.6	(kt km^{-2} a^{-1})

specific event. Therefore, flux results for the individual events can vary widely and yet all of them should have their share in the result for the flux of the total area. The mean emission for a given area is thus represented best by the sum of all observations divided by the number of observations (i.e. the arithmetic mean), and its uncertainty is given by quadratic addition of the random errors of the individual observations. Our results regarding the national CH_4 and N_2O emissions (Van der Laan et al., 2009b), for which we used the same event-based ^{222}Rn technique, but for which we presented the results based on the median and a lognormal fit, will therefore be revised according to our approach presented here (i.e. using two sectors and the arithmetic mean) in a forthcoming paper together with an extended data set. The new results for the fluxes for the Netherlands so far are given in Van der Laan (2010). They are higher by about 50% compared to the lognormal approach and still confirm the national inventories.

Of course, the reliability of our method is crucially dependent on the completeness of coverage of the area, and thus on the total number and diversity of the events. Figure 3 is encouraging in the sense that it shows that our observations cover the footprint very well. Furthermore, the results we achieved from testing our method on the simulated data from the REMO model (i.e. calculating fluxes from individual events and analysing their trajectories), fed with EDGAR $FFCO_2$ emission data and the ^{222}Rn field of Szegvary et al. (2009) are crucial, and are encouraging: our method returns what was put into the model for each sector. This clearly supports our methodology.

Our results are potentially biased towards the warmer months since we have less observations in the winter months of 2007 and 2008 (Fig. 8). We expect this potential bias however not to be significant since the results for the last, in terms of observations more nicely distributed, year (August 2008–June 2009) would only be 11% lower.

The uncertainty for our observation-based emission estimate for the Netherlands as given in Section 4 was about 23% based on the random error, calculated as explained above. For the combined uncertainty we should also consider systematic errors, related to the conversion from $\Delta^{14}C$ to $FFCO_2{}^*$ and the assumed ^{222}Rn soil emission rate. In this study the used ^{222}Rn soil flux was based on Szegvary et al. (2009). The uncertainty was estimated by the authors to be $\pm$30% for the annually mean ^{222}Rn soil flux of the Netherlands. However, Figs. 7a and b show that the modelled ^{222}Rn concentrations agree very well with our observations, suggesting, at least for the annual means, that the ^{222}Rn soil flux is representative for the Netherlands. By using two sectors, we take into account part of the spatial variation and also a small seasonal cycle in the LOESS fit (Fig. 5) was included. On small time scales the uncertainty can potentially be large, which is mostly attributed to the fact that although the production of ^{222}Rn in the soils is constant its emission is influenced by atmospheric pressure, soil temperature and soil humidity. For example, the ^{222}Rn soil flux can vary by an order of magnitude due to, for example, rain or snow and proportionally affect the calculated fluxes. This probably explains, together with the uncertainty related to the modelled transport in REMO, the large scatter in Fig. 7b. However, we expect this effect to be a minor contribution in our results as we calculated the surface fluxes per single event of which the average duration is in the order of about 10 h. For our annual mean $\Phi FFCO_2{}^*$ emissions we therefore estimate the uncertainty related to the ^{222}Rn soil flux at about 10%.

The systematic uncertainty in our $FFCO_2$ observations is directly introduced into the $dCO/FFCO_2$ ratio for which we applied a weighted harmonic fit with a linear component to calculate $\Phi FFCO_2{}^*$. The fit is mostly determined by the last 2 yr of observations since there are far less observations in the first year, and the observations we do have are subjected to relatively large uncertainties. The uncertainty in the fit is estimated to be about 20% based on the uncertainties in the amplitude and the offset. However, this fit is based on 2-weekly integrated observations of CO and $FFCO_2$ whereas our events are typically 10 h. The ratio of $dCO/FFCO_2$ could be influenced by a diurnal variation related to the fact that different fossil fuel combustion processes (e.g. domestic heating and traffic) have very different $CO/FFCO_2$ ratios, and their relative contribution varies over the day (Levin and Karstens, 2007). Another potential source of uncertainty could be biomass burning or photochemical effects (Campbell et al., 2007). More research is needed to better estimate the temporal variation in the $dCO/FFCO_2$ ratio, for example by analysing events on a high-resolution basis for CO and $FFCO_2$ by using flask samples. We do not expect this uncertainty to contribute significantly to our annually averages, but our event selection procedures could potentially introduce a bias.

Another source of uncertainty is the fact that the ^{222}Rn flux method is based on (vertical) atmospheric gradients which are observed mostly in the evenings and nights when the atmosphere is in general more stable (Fig. 10). Our method is therefore less suitable for estimating surface emissions in the afternoon when vertical mixing is more pronounced. Most of the day is, however, well covered and also the traffic peaks in the mornings and evenings are generally included in our data set. Figure 10 shows furthermore that there is no significant correlation between the height of the flux and the time of the events, which is probably because each event represents a single integrated value that usually includes emissions over several hours during day and night.

The sensitivity to the value of the correlation coefficient R as a threshold for the events was also tested: our results would be about 8% higher (but less representative due to the lower number of events) when choosing $R \geq 0.8$ as a cut-off value, and 2% lower with $R \geq 0.6$. Our results are therefore not significantly biased by our choice of R.

In total, we estimate the systematic error to be $\pm$25%. Together with our random error of 23% this leads to a combined uncertainty for our annually mean results (Table 1) of $\pm$35%.

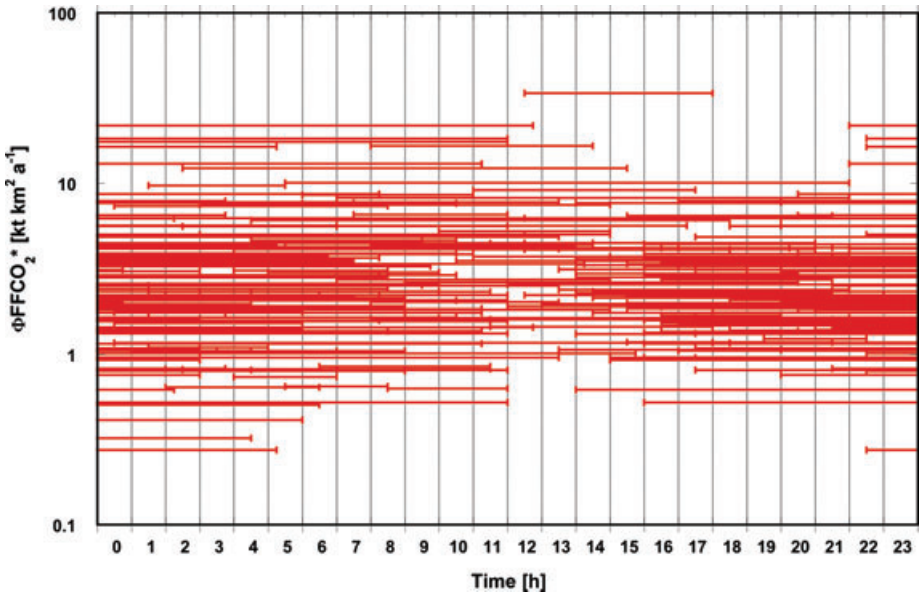

Fig. 10. Distribution of the selected events during the day. Fewer events are observed during 10:00–16:00 when vertical mixing is more pronounced.

6. Conclusions and outlook

The method presented here provides an important independent approach for validating inventories. We conclude that our method of ^{222}Rn flux approach leads to a reliable estimate ($\pm$35%) of the $\Phi FFCO_2$ fluxes for the Netherlands. For detecting year-to-year variations the uncertainty is lower ($\pm$23%). Our methodology is firmly backed-up by the simulated data treatment using REMO, for which our method reproduced the input emissions of EDGAR, and analysis of the distribution density of our observations towards the footprint. This implies that, using our method, a single monitoring station is in principle capable of determining the $\Phi FFCO_2$ flux for an area at least the size of the Netherlands (36 000 km^2). However, it is crucial that the target area is sufficiently covered by the trajectories of the collected events. Although in this sense the location of station Lutjewad is close to ideal, this requirement is ideally fulfilled with a network of monitoring stations to ensure that each grid on the total footprint is covered semi-continuously.

Based on 3 yr of observations from station Lutjewad for the period of May 2006–June 2009 we estimate net emissions for fossil fuel derived CO_2 of: (4.7 $\pm$ 1.6) kt km^{-2} a^{-1} for the Netherlands. Our result agrees very well with the Dutch inventory of (4.5 $\pm$ 0.2) kt km^{-2} a^{-1} (average value from 2006 to 2008) but more research is needed to reduce the uncertainties.

As a side result we found that the ^{222}Rn soil flux estimates of Szegvary et al. (2009) are representative for the Netherlands. Still, for future studies we suggest more research to further constrain the ^{222}Rn soil flux. If future research would result in a more reliable soil ^{222}Rn emanation rate, our values can be adjusted in a simple way as they are directly proportional to this emission rate. We encourage that our method is applied using data from other stations. We suggest that the sensitivity towards specific regions (i.e. how each grid is covered) is tested with a higher resolution forward transport model in combination with a high-resolution emission inventory (e.g. the newly available $0.1^\circ \times 0.1^\circ$ EDGAR4.0 database). For each individual event the surface fluxes could then be calculated based on its individual trajectory.

7. Acknowledgments

This project has been cofunded by the Dutch national research programme Climate changes Spatial Planning (CcSP), project ME2 'Integrated observations and modelling of Greenhouse Gas budgets at the national level in the Netherlands', and by the EU FP6- project CarboEurope-IP (contract nr. GOCE-CT-2003–505572).

The authors would like to thank: H.J. Streurman, B.A.M. Kers, J.C. Roeloffzen, J.K. Schut and E. Kettner for technical assistance, Y. Huismans for assistance with Matlab, A.T. Vermeulen for fruitful discussions, C. Gerbig for providing the temporal extrapolation of the emission data and I. Levin for supplying the Δ^{14}C data from station Jungfraujoch. We are grateful for the efforts of the three reviewers whose comments provided significant contributions to this paper.

References

Baker, D. F., Law, R. M., Gurney, K. R., Rayner, P., Peylin, P. and co-authors. 2006. TransCom 3 inversion intercomparison: impact of transport model errors on the interannual variability of regional CO_2 fluxes, 1988–2003. *Glob. Biogeochem. Cycle* **20**, 17.

Bergamaschi, P., Krol, M., Dentener, F., Vermeulen, A., Meinhardt, F. and co-authors. 2005. Inverse modelling of national and European CH4 emissions using the atmospheric zoom model TM5. *Atmos. Chem. Phys.* **5**, 2431–2460.

Bousquet, P., Peylin, P., Ciais, P., Le Quere, C., Friedlingstein, P. and co-authors. 2000. Regional changes in carbon dioxide fluxes of land and oceans since 1980. *Science* **290**, 1342–1346.

Campbell, J. E., Carmichael, G. R., Tang, Y., Chai, T., Vay, S. A. and co-authors. 2007. Analysis of anthropogenic CO_2 signal in ICARTT using a regional chemical transport model and observed tracers. *Tellus B* **59**, 199–210.

Draxler, R. R. and Rolph, G. D. 2003. HYSPLIT (HYbrid Single-Particle Lagrangian Integrated Trajectory) Model access via NOAA ARL READY Website (http://www.arl.noaa.gov/ready/hysplit4.html). NOAA Air Resources Laboratory, Silver Spring, MD.

Engelen, R. J., Denning, A. S. and Gurney, K. R. 2002. On error estimation in atmospheric CO_2 inversions. *J. Geophys. Res.* **107**, 4635, doi:10.1029/2002JD002195.

Forster, P., Ramaswamy, V., Artaxo, P., Berntsen, T., Betts, R. and co-authors. 2007. Changes in Atmospheric Constituents and in Radiative Forcing. In: *Climate Change 2007: The Physical Science Basis. Contribution of Working Group I to the Fourth Assessment Report of the Intergovernmental Panel on Climate Change* (eds Solomon, S., D. Qin, M. Manning, Z. Chen, M. Marquis and co-editiors). Cambridge University Press, Cambridge, United Kingdom and New York, NY, USA.

Gamnitzer, U., Karstens, U., Kromer, B., Neubert, R. E. M., Meijer, H. A. J. and co-authors. 2006. Carbon monoxide: a quantitative tracer for fossil fuel CO_2? *J. Geophys. Res.* **111**, D22302, doi:10.1029/2005JD006966.

Graven, H. D., Stephens, B. B., Guilderson, T. P., Campos, T. L., Schimel, D. S. and co-authors. 2009. Vertical profiles of biospheric and fossil fuel-derived CO_2 and fossil fuel CO_2:CO ratios from airborne measurements of ^{14}C, CO_2 and CO above Colorado, USA. *Tellus* **61B**, 536–546.

Hesshaimer, V. 1997. *Tracing the global carbon cycle with bomb radiation*. PhD thesis. Univ. of Heidelberg, Heidelberg, Germany.

Langmann, B. 2000. Numerical modelling of regional scale transport and photochemistry directly together with meteorological processes. *Atmos. Environ.*, 3585–3598.

Levin, I. 1984. *Atmospheric CO_2, sources and sinks on the European continent (in German)*. PhD Thesis. Univ. of Heidelberg, Heidelberg, Germany.

Levin, I. 1987. Atmospheric CO_2 in continental Europe—an alternative approach to clean air CO_2 data. *Tellus* **39B**, 21–28.

Levin, I., Kromer, B., Schmidt, M. and Sartorius, H. 2003. A novel approach for independent budgeting of fossil fuel CO_2 over Europe by $^{14}CO_2$ observations. *Geophys. Res. Lett.* **30**, 2194, doi:10.1029/2003GL018477.

Levin, I. and Karstens, U. 2007. Inferring high-resolution fossil fuel CO_2 records at continental sites from combined $^{14}CO_2$ and CO observations. *Tellus* **59B**, 245–250.

Levin, I., Hammer, S., Kromer, B. and Meinhardt, F. 2008. Radiocarbon observations in atmospheric CO_2: Determining fossil fuel CO_2 over Europe using Jungfraujoch observations as background. *Sci. Tot. Environ.* **391**, 211–216.

Meijer, H. A. J., Smid, H. M., Perez, E. and Keizer, M. G. 1996. Isotopic characterisation of anthropogenic CO_2 emissions using isotopic and radiocarbon analysis. *Phys. Chem. Earth* **21**, 483–487.

Mook, W. G. and Van Der Plicht, J. 1999. Reporting ^{14}C activities and concentrations. *Radiocarbon* **41**, 227–239.

Neubert, R. E. M., Spijkervet, L. L., Schut, J. K., Been, H. A. and Meijer, H. A. J. 2004. A computer-controlled continuous air drying and flask sampling system. *J. Atmos. Ocean Tech.* **21**, 651–659.

Olivier, J. G. J., Van Aardenne, J. A., Dentener, F., Ganzeveld, L. and Peters, J. A. H. W. 2005. Recent trends in global greenhouse gas emissions: regional trend and spatial distribution of key sources. In: *"Non-CO_2 Greenhouse Gases (NCGG-4)". A. van Amstel (coord.)*, pp.325–330. Millpres, Rotterdam, ISBN 9059660439.

Peylin, P., Rayner, P. J., Bousquet, P., Carouge, C., Hourdin, F. and co-authors. 2005. Daily CO_2 flux estimates over Europe from continuous atmospheric measurements: 1, inverse methodology. *Atmos. Chem. Phys.* **5**, 3173–3186.

Randerson, J. T., Enting, I. G., Schuur, E. A. G., Caldeira, K. and Fung, I. Y. 2002. Seasonal and latitudinal variability of troposphere $^{14}CO_2$: post bomb contributions from fossil fuels, oceans, the stratosphere, and the terrestrial biosphere. *Global Biogeochem. Cycle* **16**, 1112, doi:10.1029/2002GB001876.

Rayner, P. J., Enting, I. G., Francey, R. J. and Langenfelds, R. 1999. Reconstructing the recent carbon cycle from atmospheric CO_2, delta ^{13}C and O_2/N_2 observations. *Tellus B* **51**, 213–232.

Rödenbeck, C., Houweling, S., Gloor, M. and Heimann, M. 2003. CO_2 flux history 1982–2001 inferred from atmospheric data using a global inversion of atmospheric transport. *Atmos. Chem. Phys.* **3**, 1919–1964.

Rödenbeck, C., Conway, T. J. and Langenfelds, R. L. 2006. The effect of systematic measurement errors on atmospheric CO_2 inversions: a quantitative assessment. *Atmos. Chem. Phys.* **6**, 149–161.

Rypdal, K. and Winiwarter, W. 2001. Uncertainties in greenhouse gas emission inventories—evaluation, comparability and implications. *Environ. Sci. Policy* **4**, 107–116.

Schmidt, M., Graul, R., Sartorius, H. and Levin, I. 1996. Carbon dioxide and methane in continental Europe: a climatology, and ^{222}Radon-based emission estimates. *Tellus* **48B**, 457–473.

Stuiver, M. and Polach, H. 1977. Reporting of ^{14}C data. *Radiocarbon* **19**, 355–363.

Szegvary, T., Conen, F. and Ciais, P. 2009. European ^{222}Rn inventory for applied atmospheric studies. *Atmos. Environ.* **43**, 1536–1539.

Thom, M., Bösinger, R., Schmidt, M. and Levin, I. 1993. The Regional Budget of Atmospheric Methane of a Highly Populated Area. *Chemosphere* **26**, 143–160.

Tolk, L. F., Meesters, A., Dolman, A. J. and Peters, W. 2008. Modelling representation errors of atmospheric CO_2 mixing ratios at a regional scale. *Atmos. Chem. Phys.* **8**, 6587–6596.

Turnbull, J. C., Miller, J. B., Lehman, S. J., Tans, P. P., Sparks, R. J. and co-authors. 2006. Comparison of $^{14}CO_2$, CO, and SF_6 as tracers for recently added fossil fuel CO_2 in the atmosphere and implications for biological CO_2. *Geophys. Res. Lett.* **33**.

UNFCCC 2009. United Nations Framework Convention on Climate Change, national reports. Available at: http://unfccc.int/national_reports/items/1408.php.

Van Der Laan, S., Neubert, R. E. M. and Meijer, H. A. J. 2009a. A single gas chromatograph for atmospheric mixing ratio

measurements of CO_2, CH_4, N_2O, SF_6 and CO. *Atmos. Meas. Tech.* **2**, 549–559.

Van Der Laan, S., Neubert, R. E. M. and Meijer, H. A. J. 2009b. Methane and nitrous oxide emissions in The Netherlands: ambient measurements support the national inventories. *Atmos. Chem. Phys.* **9**, 9369–9379.

Van Der Laan, S. 2010. *Validation of the Greenhouse Gas Balance of The Netherlands, Observational constraints on CO_2, CH_4 and N_2O from atmospheric monitoring station Lutjewad*. PhD thesis. Centre for Isotope Research, University of Groningen, Groningen, Netherlands.

Whittlestone, S. and Zahorowski, W. 1998. Baseline radon detectors for shipboard use: development and deployment in the First Aerosol Characterization Experiment (ACE 1). *J. Geophys. Res.* **103**(D13), 16743–16751.

Zondervan, A. and Meijer, H. A. J. 1996. Isotopic characterisation of CO_2 sources during regional pollution events using isotopic and radiocarbon analysis. *Tellus* **48B**, 601–612.